Filler Metal Influence on the Weld Metal Structure of 25Cr-35Ni Heat Resistant Steel

A. Asadollahi[1], A. Bahrami*[2], M. Shamanian[3]

Department of Materials Engineering, Isfahan University of Technology, Isfahan 84156-83111, Iran

Abstract

This paper investigates the effects of 25Cr-35Ni and 35Cr-45Ni filler metals on the weldability, microstructure, and mechanical properties of 25Cr-35Ni heat-resistant steel. The 25Cr-35Ni alloy is known to have excellent high-temperature properties, such as creep resistance and high-temperature corrosion/oxidation resistance, making this grade an ideal option for demanding high-temperature applications in oil, gas, and petrochemical industries. Gas tungsten arc welding is a routine practice for the repair and joining of components, made of heat resistant steel. Microstructure and mechanical properties of welded samples with 25Cr-35Ni and 35Cr-45Ni filler metals were studied using optical microscopy, electron microscopy, and tensile and hardness tests. Fractography of fracture surfaces was also conducted, using an electron microscope. Results show that the microstructure in the heat-affected zone area in both cases is primarily affected by the heat input during melting. A noticeable carbide dissolution was observed in both cases. In neither of filler metals was there any indication of sigma phase formation in the weld, which is related to the high nickel content of filler metals. Results also showed that the heat-affected zone controls mechanical properties in both cases.

Keywords: 25Cr-35Ni heat resistant steel; Welding; Mechanical properties.

1. Introduction

Heat-resistant alloys and more specifically 25Cr-35Ni alloy, known as HP alloy, are widely used for high-temperature applications in oil, gas, and petrochemical industries, since these alloys exhibit superior high-temperature mechanical properties, outstanding structural stability during high-temperature service conditions, and excellent high-temperature corrosion/oxidation resistance [1-3]. HP alloys, for instance, are widely used in reformer tubes, radiant tubes, and gas turbine components [4-11], which are designed to work in temperatures over 650 up to 1100 ºC.

Cracking and reforming furnaces are critical units in petrochemical plants, as the working conditions are often very aggressive and severe. These alloys, expected to perform in high-temperature applications, must have excellent corrosion resistance, oxidation resistance, and high temperature creep strength. These steels are exposed to very harsh conditions such as high temperatures and the existence of oxidizing, nitriding and carburizing gases.

Superior high-temperature properties of HP alloys root back into their chemical compositions. HP alloys contain high nickel and chromium concentrations, with the latter known as a strong carbide former. In addition, these alloys typically have some Nb or Ti in their compositions, which form stable titanium/niobium carbides re-

**Corresponding author*
Email:a.n.bahrami@iut.ac.ir
Address: Department of Materials Engineering, Isfahan University of Isfahan P.O.box:84156-83111, Iran
1. M.Sc.
2. Assistant Professor
3. Professor

sulting in an improved creep resistance [12]. The excellent creep resistance of HP alloys has to do with the formation of a network of eutectic chromium carbides together with fine inter-dendritic secondary titanium/niobium carbides, formed during heat treatment [10-12]. Long-term continuous high-temperature service exposure of HP alloys results in the coarsening of fine precipitates, resulting in the deterioration of creep resistance of these alloys. Controlling microstructure and precipitates is crucial when enhancing the creep resistance, and high-temperature mechanical properties of HP alloys are significant concerns [12-14]. This becomes even more crucial when it comes to components, containing welding. In many industrial applications, HP alloys are welded. Besides, repair welding of these alloys is also a common industrial practice. There is limited information on the effects of filler metals on the microstructure and mechanical properties of HP alloys. Obviously, it is best to have a matching filler to increase the integrity of the joint. However, different filler metals can also be employed if a specific property is expected from the joint (e.g. higher creep or thermal shock resistance, compared to the base metal). This paper compares the weldability, microstructure, and mechanical properties of HP alloys, in case 25Cr-35Ni and 35Cr-45Ni filler metals are used. The latter filler metal has higher contents of Cr and Ni, making it a better option, when creep resistance is the primary concern. This paper compares the microstructure and mechanical properties of HP alloy joints, welded with 25Cr-35Ni and 35Cr-45Ni filler metals.

2. Materials and methods

In this investigation, the alloy is a cast 25Cr-35Ni alloy, taken from a spun cast reformer tube with an outer diameter of 130 mm and thickness of 20 mm. The chemical composition of the alloy and those of 25Cr-35Ni and 35Cr-45Ni filler metals are given in Table 1. Sample dimensions are 10x5x2 cm^3. Samples are beveled with an angle of 50º, according to ASME section IX. Without pre-heating, specimens were welded with gas tungsten arc welding, using direct current

electrode negative (DCEN). The diameter of filler rods was 2.4 mm. More details of welding specifications are given in Table 2. The microstructure of welded samples was studied using optical and electron microscopes. Mechanical properties of samples were evaluated using tensile and Vickers microhardness tests. The tensile test was carried out according to standard ASTM-E8. Optical and electron microscopes were used to study the microstructure of samples. Metallography samples were prepared with grinding using grinding papers 80 to 2000, followed by polishing with alumina paste. Samples were then etched for 10 s with a solution, containing 10 $CuSO_4$, 50 cc HCl, and 50 cc water. The microstructure of welded samples was also characterized using energy-dispersive X-ray spectroscopy.

3. Results and discussions

Optical and electron microscope micrographs of the

Table 1. Chemical compositions of base alloy and filler metals.

Composition	Ni	Cr	C	Mn	Si	Nb	Mo	Fe
Base Metal	35.8	24.4	0.4	1.35	1.3	1.3	0.04	Bal.
Filler 25-35 (Sample 1)	35.2	25.5	0.4	1.59	1.0	1.2	-	Bal.
Filler 35-45 (Sample 2)	45.5	35.0	0.42	1.0	1.5	0.8	-	Bal.

Table 2: Welding parameters.

Welding parameters	Filler 25Cr-35Ni (Sample 1)		Filler 35Cr-45Ni (Sample 2)	
	1st Pass	Next Passes	1st Pass	Next Passes
Current (A)	90	130	90	130
Voltage (V)	15	15	15	15
Welding speed (1/mm)	1	1	0.8	0.8
Heat input (J/mm)	945	1365	1181	1706

as-cast microstructure of the HP specimen are presented in Figure 1. The average grain size is around 40 µm. As can be seen, grain boundaries are heavily decorated with a connected network of carbides. The distribution of fine carbides inside grains is also clearly visible. Some large blocky carbides, with their size ranging from a few micrometers up to 20 µm, are also observed. Overall, carbides can be categorized into grayish carbides and white ones. The latter appears to be less continuous, while the former carbides often appear as a continuous grain boundary phase. EDS analyses of gray and white phases, from the spots, shown in Figure 1d, are presented in Figure 2. Results depict that the gray phase is a chromium-rich carbide and the white one is a niobium-rich carbide. It is postulated that chromium-rich carbides have either $M_{23}C_6$ or M_7C_3 stoichiometry, with the former being more frequent [4,6]. Cr-rich $M_{23}C_6$ carbides can form as a result of eutectic phase transformation, in which case they are referred to as primary carbides, or they can form during heat treatment or high-temperature service exposure. In this case, they are more known as secondary carbide particles. Secondary $M_{23}C_6$ carbide particles are comparatively much smaller and are distributed more inside grains. Nb-rich carbides, on the other hand, have MC stoichiometry. They are much more stable compared to chromium-rich carbides. They are known as carbides with very slow kinetics of dissolution/coarsening. That is why niobium was added to heat resistant steels in the first place. Needless to mention that the higher the stability of carbides, the longer service time can be attained. As far as the morphology of carbides is concerned, it can be concluded that primary Cr-rich carbides have more continuity and are more distributed at grain boundaries. In contrast, Nb-rich MC carbides are finer particles, distributed over grain boundaries and inside grains.

Stereomicroscopic images of welded specimens are presented in Figure 3. In both samples, welding was carried out with seven passes together with a root pass. As can be seen, there is hardly any discontinuity, macrocracks, voids, or other irregularities in the weldments. The microstructures of different regions of welded samples, including the base metal, heat affected zone (HAZ) and welded zone, are compared, Figure 4. The welded structure is expectedly a dendritic structure in which dendrites show directional growth. There is hardly any difference between the structure of the weld in both cases, Figure 4a and 4b. Moving further away from the weld structure towards the base metal, one can clearly distinguish

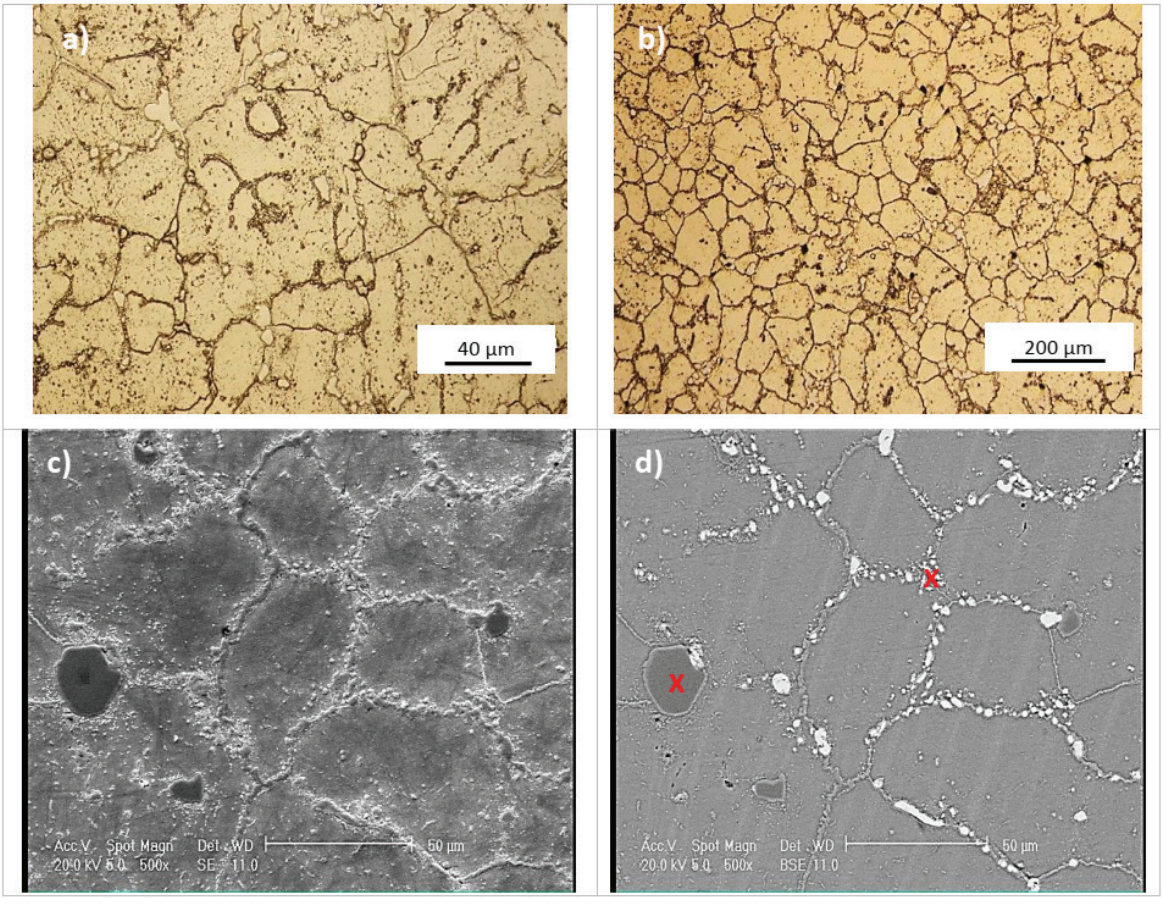

Fig. 1. Microstructure of as-cast specimens: a,b) optical microscope and c,d) SEM images.

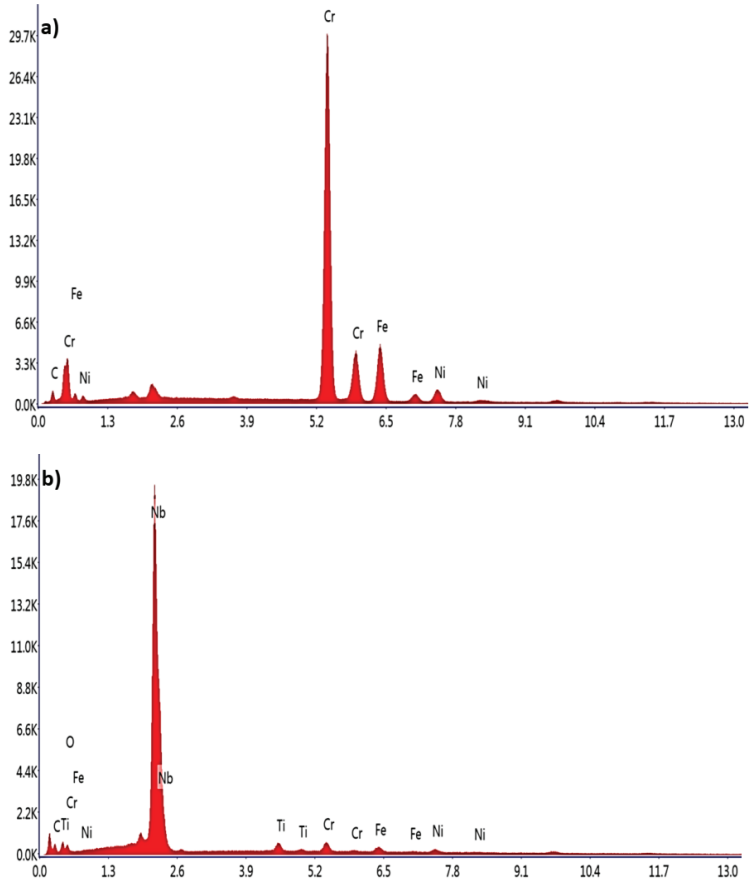

Fig. 2. EDS analyses of a) gray and b) white phases (x-axis: KeV, y-axis: Intensity (a.u.)).

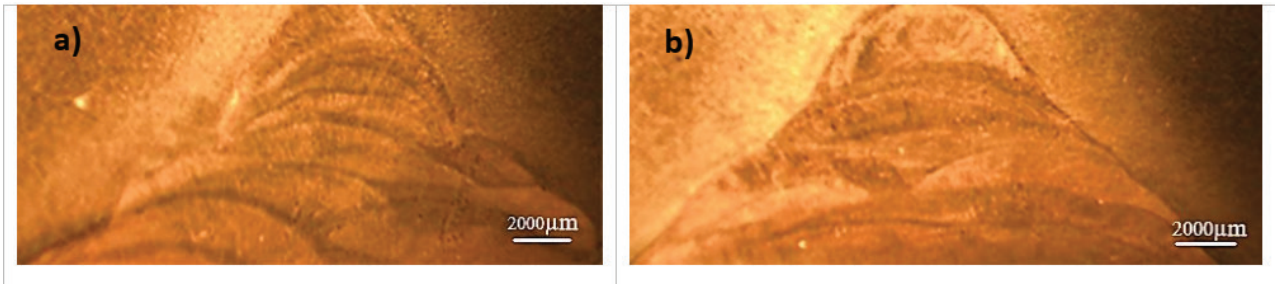

Fig. 3. Stereomicroscope images of a cross-section of a) sample #1, and b) sample #2.

between the HAZ and base metal structures. In the former, the continuously connected network of coarse carbides at grain boundaries does not exist anymore, inferring that these carbides at the heat-affected zone have been partially dissolved during welding. Moreover, sample #2 (35Cr-45Ni filler) also appears to have a comparatively slightly wider heat affected zone area than sample #1. The same applies to the grain size, i.e. the grain size at the heat-affected zone of sample #2 is slightly larger than that of sample #1. In both cases, there is an increase in the grain size in the heat-affected zone area, compared to the base metal, having to do with the heat input during welding and the partial dissolution of carbides. Carbides are known to have a pinning effect on the moving grain boundaries. Therefore, the higher the dissolution of carbides, the easier the grain boundary movement is, which leads to grain growth at the heat-affected zone area.

The electron and optical microscope micrographs of the heat-affected zone structure in samples #1 and #2 at higher magnification are presented in Figure 5. Carbides in these two samples have different morphologies. As can be seen, the remaining chromium carbides at grain boundaries in sample #1 are relatively continuous, whereas those in sample #2 are more in the form of connected large blocky carbides. Overall, carbides in sample #2 are comparatively coarser. It is due to the higher melting point of sample filler metal #2.

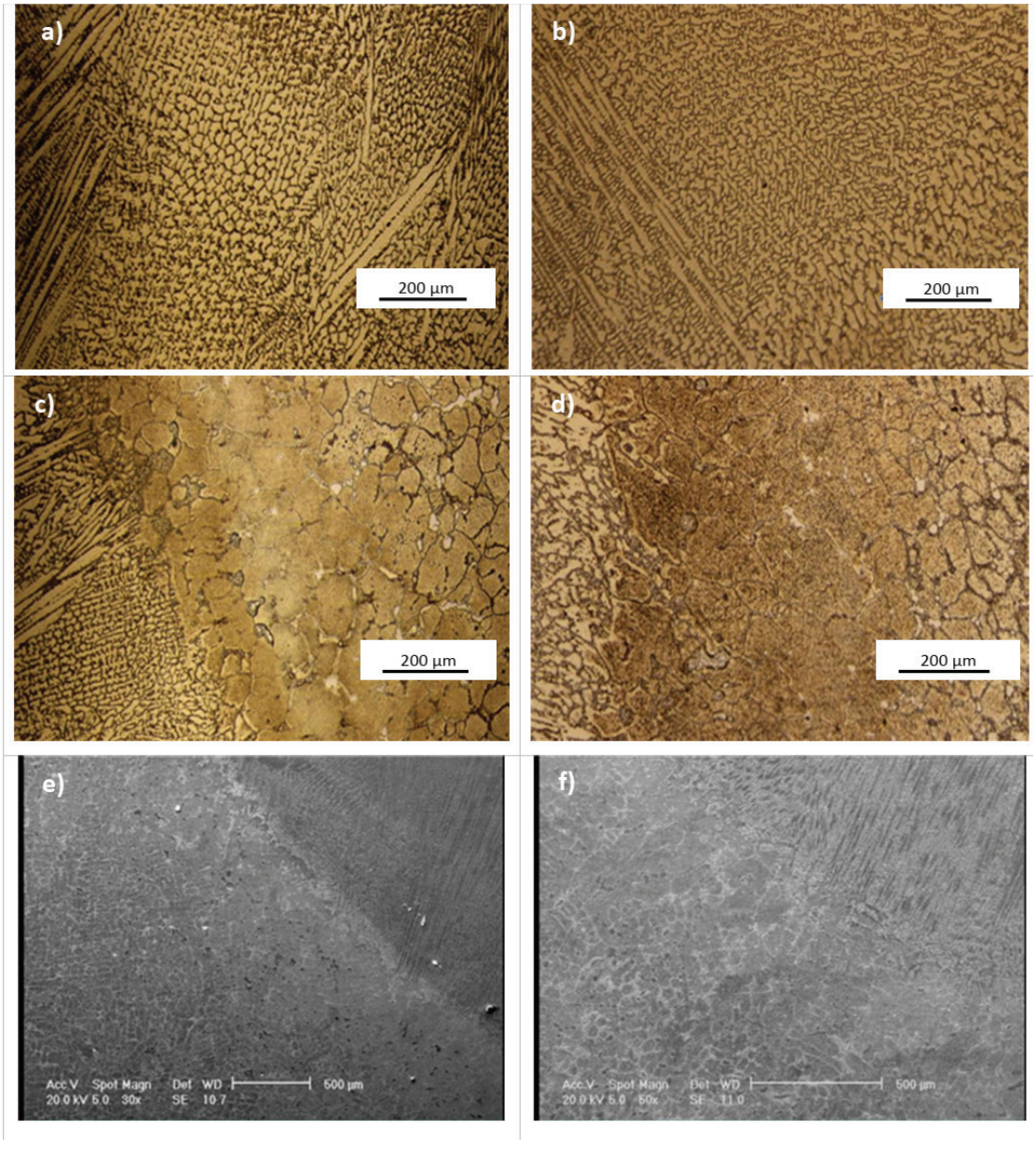

Fig.4. Microstructure of different regions of the welded samples for a, c, e) sample #1 and b, d, f) sample #2.

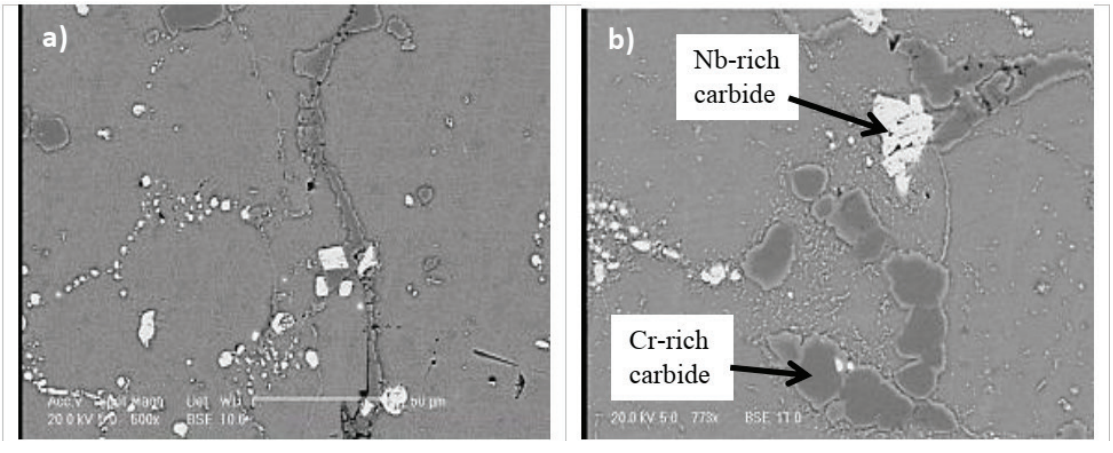

Fig. 5. Heat affected zone structure in a) sample #1 and b) sample #2.

EDS line scans of alloying elements from the base metal towards the weld are presented in Figure 6. In the case of sample #1, there is hardly any change in the alloy composition, moving from the base metal towards the weld. It has to do with the fact that in sample #1, the filler metal is similar to the base metal. On the contrary, there is a relatively sharp increase in Ni and Cr contents, moving from the base metal to the weld in sample #2, which is again related to the filler metal composition. There is no abnormality in the distribution of alloying elements across the weldment in either case.

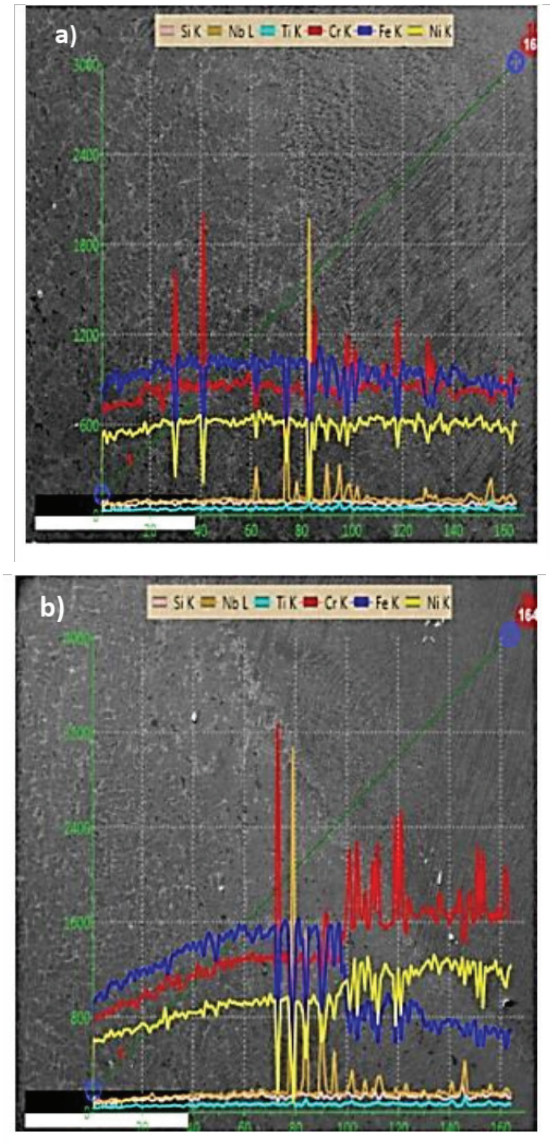

Fig. 6. EDS line scan analysis from the base metal to the weld center in a) sample #1 and b) Sample #2.

The results of the tensile tests of the specimens are presented in Table 3. Since the fracture in both specimens occurred adjacent to the weld region, the mechanical properties of the samples are approximately the same. Interestingly, the elongation of both welded samples is significantly higher than that of the as-cast specimen. While elongation in welded specimens is approximately 18 %, that in the as-cast sample is 12 %. It can be attributed to grain boundary carbides in welded specimens being less continuous. The presence of a continuous thick carbide phase at grain boundaries provides an easy path for crack propagation, which, in turn, deteriorates the ductility of specimens.

Table 3. Mechanical properties of samples.

Samples	UTS (MPa)	Elongation (%)
#1	516	18.6
#2	512	18
As-cast	517	12

An example of fracture surface in sample #1 is shown in Figure 7. Fractography results depict that fracture surfaces in both samples #1 and #2 are very similar. There are two main features, observed in fracture surfaces: i) grain boundary de-cohesion/fracture, and ii) cuasi-cleavage fracture inside grains (Cuasi-cleavage is a fracture mode that combines the characteristics of cleavage fracture and dimpled rupture fracture). It is noticeable that grain boundary de-cohesion controls the fracture, because grain boundaries provide an easy propagation path for cracks.

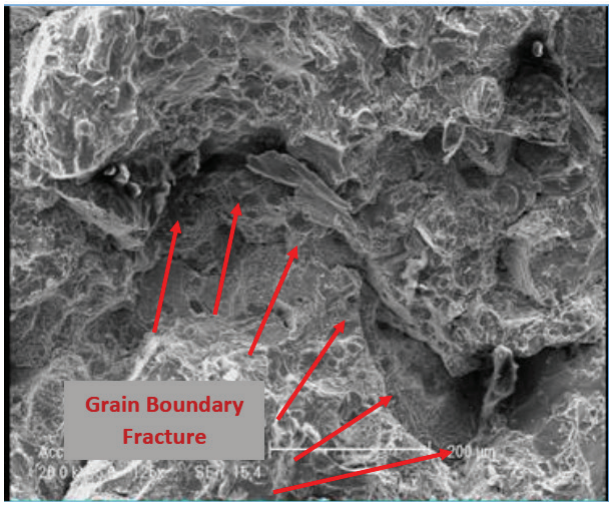

Fig. 7. Typical fracture surface in welded specimen #1.

The results of the microhardness profilometry from the center of the weld metal to the base metal are presented in Figure 8. As can be seen, there is not much of a big difference between sample #1 and sample #2, which is in accordance with the reported data on the tensile properties of samples. In addition, results indicate a significant drop in the hardness of both samples in the heat-affected

zone area. It can be explained by the fact that there is a massive carbide dissolution in the heat-affected zone of both samples and that there is a slight grain growth in the heat-affected zone as well. It is also noteworthy that the width of heat affected zone in sample #2 is relatively slightly more extensive than that of sample #1, which is again in agreement with the microscopic data reported earlier in this paper.

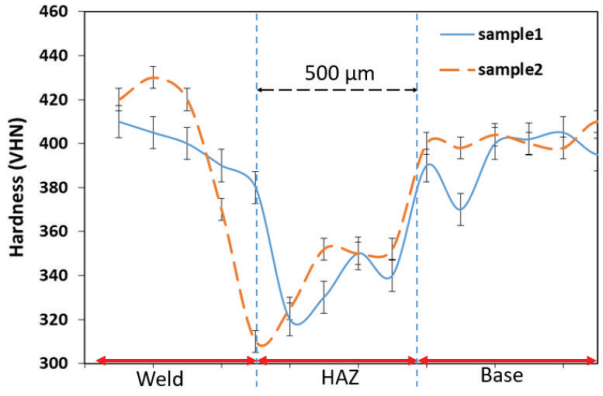

Fig. 8. Hardness profilometry across the weldment.

4. Discussion

Tubes in cracking furnaces for high-temperature applications must have corrosion resistance, oxidation resistance and high-temperature strength. These tubes are exposed to very harsh conditions such as high temperatures and the existence of oxidizing, nitriding and carburizing gases. Austenitic alloys are widely used in various applications at high temperatures due to their structural stability, relatively good mechanical properties at high temperatures and corrosion resistance. These alloys contain large amounts of carbide-forming elements in their chemical composition, which leads to the formation of small inter-dendritic carbides uniformly in structure. Among various austenitic alloys, alloys with relatively high levels of chromium and nickel in their composition are commonly used to make cracking tubes. The optimal life of these tubes is approximately 100,000 hours if they are exposed to temperatures above 850 °C. According to researches and observations, oxidation and carburization reactions typically occur after 10,000 hours of operation, and their microstructure changes. The microstructure and surface coating of these alloys play an important role in their lifetimes [15,16]. HP alloys are widely used in different petrochemical plants, including steam-reforming units, among other heat-resistant alloys. Reformers are expected to work in severe high-temperature working conditions. The service life of reformer tubes has a significant impact on the functionality and profitability of a petrochemical plant. Unexpected failures in reformer and radiant tubes imposes tremendous costs on the working systems [17]. Given that pipes and elbows are welded in a reformer unit, it is vital to have an in-depth understating of the microstructure and mechanical properties of welded HP tubes. This paper investigates the effects of 25Cr-35Ni and 35Cr-45Ni filler metals on the weldability, microstructure, and mechanical properties of 25Cr-35Ni heat resistant steel. These two filler metals are routinely used for welding and repairing radiant tubes in reforming installations. Results show that the microstructure of HP alloy is essentially an equiaxed grain structure with the distribution of carbides at the grain boundaries and inside grains. Carbides can be categorized into chromium-rich $M_{23}C_6$ carbides in the form of either primary carbides or secondary carbides and niobium-rich carbides, with MC stoichiometry. Niobium carbides are very stable with very slow kinetics of dissolution/coarsening. Results also showed that Cr-rich carbides have more continuity and are more distributed at grain boundaries, whereas Nb-rich carbides are more in the form of fine particles. Welding by both filler metals has significant implications for the structure of HP alloy in the heat-affected zone area. There is a significant carbide dissolution in the HAZ of both cases, resulting in a great reduction in the carbide content of the alloy in the heat-affected zone structure. The morphology of remaining carbides in the HAZ of the alloy is slightly different in these two samples. In the case of filler metal 25Cr-35Ni, the remaining carbides are more in the form of a thick layer at the grain boundary, whereas filler metal 35Cr-45Ni is more in the form of connected blocky carbides. Partial dissolution of carbides in both cases has resulted in slight grain growth. That in case of the latter filler metal (35Cr-45Ni) is marginally higher. Carbide dissolution and grain growth in the heat-affected zone structure results in a significant drop in the hardness of the alloy in the heat-affected zone area. Results also showed that different areas of welded samples show a complete bonding with no crack, de-bonding, or other abnormalities, inferring that the weldability of HP alloy with both filler metals is excellent. It is due to the high percentage of nickel in both filler metals that prevents the formation of the sigma phase [18] and cracks in the weldment. Also, base metal ductility is one of the reasons for the great weldability of HP alloys in casting conditions. The great ductility of HP alloy enables plastic deformation during cooling after welding, which minimizes the risk of crack formation during and after welding. This great compatibility between the base and filler metals is reflected in the mechanical properties of the joints, as the mechanical properties of welded specimens are very similar to those of as-cast alloy. The fractography results showed that the fracture mode in both cases is a combination of the causi-cleavage and grain boundary de-cohesion. The latter has to do with a thick carbide layer at grain boundaries which provides an easy crack propagation path. As far as the structure at the weldment is concerned, the structure in both cases is a typical dendritic

structure. It is seen that the distance between the dendritic arms in the case of filler 35Cr-45Ni is higher than that in the case of filler 25Cr-35Ni, having to do with the higher heat input in the former case. This roots back to the fact that filler 35Cr-45Ni has a higher melting point. This also results in a slightly wider heat affected zone area as well as a comparatively coarser grain structure in the sample with filler 35Cr-45Ni.

5. Conclusions

This paper investigates the effects of filler metals 25Cr-35Ni and 35Cr-45Ni on the microstructure, and mechanical properties of gas tungsten arc welded HP alloy. The following conclusions can be drawn from the results obtained in this investigation:

- Excellent weldability was observed in both 25Cr-35Ni and 35Cr-45Ni filler metals. Hardly was there any crack or discontinuity in the weldments. It is attributable to the high nickel content in both fillers.
- In both cases, the heat-affected zone structure is influenced mainly by the heat input during welding. Carbides, for instance, are dissolved to a large extent. There is a grain growth in both samples as well.
- Remaining carbides in the heat-affected zone area in the case of filler 25Cr-35Ni are more in the form of a continuous thick layer at grain boundaries. In contrast, those in filler 35Cr-45Ni filler have blocky morphologies.
- The width of the heat-affected zone area and average grain size in the heat-affected zone in the case of filler 35Cr-45Ni is slightly larger than that in filler 25Cr-35Ni. The higher heat input can explain it in the former case due to the higher melting point of filler 35Cr-45Ni.
- Carbide dissolution and grain growth in the heat-affected zone area is associated with a drop in the hardness profile across the weldment in both samples.
- Mechanical properties in both fillers are very similar, inferring that the damage in both cases is controlled with heat affected zone area.

Reference

[1] M. Attarian, A. Karimi Taheri, S. Jalilvand, A. Habibi: Eng. Fail. Anal. 68 (2016) 32.

[2] M.J. Donachie, S.J. Donachie, Superalloys: 2nd Ed. ASM Int. A Technical Guide, United States of America, 2002.

[3] R. Dehmolaei, M. Shamanian, A. Kermanpur: Sci. Tech. Weld. Join. 12(7) (2007), 586.

[4] X.Q. Wu XQ, H.M. Jing, Y.G. Zheng, Z.M. Yao, W. Ke, Z.Q. Hu: Mater. Sci. Eng. 293(1-2) (2000), 252.

[5] K.S. Guan, F. Xu, Z.W. Wang, H. Xu: Eng. Fail. Anal. 12(1) (2004), 1.

[6] R. Dehmolaei, M. Shamanian, A. Kermanpur: Sci. Tech. Weld. Join. 13(6) (2008), 515.

[7] M. Attarian, A. Karimi Taheri: Mater. Sci. Eng. 659(6) (2016), 104.

[8] S. Shi, J.C. Lippold: Mater. Charac. 59(8) (2008), 1029.

[9] R. Dehmolaei, M. Shamanian, A. Kermanpur: Mater. Charac. 59(12) (2018), 1814.

[10] ASM Handbook "Castings", Metals Park, OH: ASM International, 15 (1988) 727.

[11] R.M.T. Borges, L.H. de Almeida: Acta Microscopy Supply A. 8 (1999) 251.

[12] A. Bahrami, P. Taheri, Metals. 2019.

[13] G.D.A. Soares, L.H. de Almeida, T.L. da Silveira, I.L. May: Mater. Charac. 29(3) (1992), 387.

[14] S.J. Zhu, P.E. Li, J. Zhao, Z.B. Cao: Mater. Sci. Eng. 114 (1989) 7.

[15] M. Taghipour, A. Bahrami, R. Rahimzadeh, V. Esmaeili: J. Fail. Anal. Prev. (2021) 1-11.

[16] M. Taghipour, A. Eslami, M. Salehi, A. Bahrami: Surface Coatings Tech. 389 (2020), 125607

[17] H. Pourmohammad, A. Bahrami, A. Eslami, M. Taghipour: Eng. Fail. Anal. 104 (2019), 216.

[18] A. Bahrami, A. Ashrafi, S.M. Rafiaei, M. Yazdan Mehr: Eng. Fail. Anal. 82 (2017) 56.